Novel quinazoline–urea analogues as modulators for Aβ-induced mitochondrial dysfunction: Design, synthesis, and molecular docking study

ARTICLE *in* EUROPEAN JOURNAL OF MEDICINAL CHEMISTRY · SEPTEMBER 2014

Impact Factor: 3.45 · DOI: 10.1016/j.ejmech.2014.07.027

6 AUTHORS, INCLUDING:

Ahmed Elkamhawy
Korea Institute of Science and Technology
14 PUBLICATIONS **5** CITATIONS
SEE PROFILE

Ae Nim Pae
Korea Institute of Science and Technology
179 PUBLICATIONS **1,492** CITATIONS
SEE PROFILE

European Journal of Medicinal Chemistry 84 (2014) 466–475

Contents lists available at ScienceDirect

European Journal of Medicinal Chemistry

journal homepage: http://www.elsevier.com/locate/ejmech

Original article

Novel quinazoline-urea analogues as modulators for Aβ-induced mitochondrial dysfunction: Design, synthesis, and molecular docking study

Ahmed Elkamhawy [a, b], Jiyoun Lee [c], Beoung-Geon Park [d, e], Insun Park [e, f], Ae Nim Pae [e], Eun Joo Roh [a, b, *]

[a] Chemical Kinomics Research Center, Korea Institute of Science and Technology (KIST), Seoul 136-791, South Korea
[b] Department of Biological Chemistry, Korea University of Science and Technology (UST), Daejeon 305-350, South Korea
[c] Department of Global Medical Science, Sungshin Women's University, Seoul 142-732, South Korea
[d] School of Life Sciences and Biotechnology, Korea University, Seoul 136-701, South Korea
[e] Center of Neuromedicine, Korea Institute of Science and Technology (KIST), Seoul 136-791, South Korea
[f] Department of Biotechnology, Yonsei University, Seoul 120-749, South Korea

ARTICLE INFO

Article history:
Received 12 April 2014
Received in revised form
4 July 2014
Accepted 8 July 2014
Available online 9 July 2014

Keywords:
Mitochondrial permeability transition pore (mPTP)
Alzheimer's disease (AD)
Quinazoline-urea
Cyclophilin D (CypD)
β-amyloid peptide (Aβ)
Molecular docking

ABSTRACT

A novel series of twenty-six quinazoline-urea derivatives was designed and synthesized. Their blocking activities against β-amyloid peptide (Aβ) induced mitochondrial permeability transition pore (mPTP) opening were evaluated by JC-1 assay which measured the change of mitochondrial membrane potential. Seven compounds showed better inhibitory activities than the standard Cyclosporin A (CsA). The most active analogues were tested by MTT assay to evaluate their toxicity on the cellular survival; they revealed excellent cellular viability. To explain the difference in inhibitory activity, molecular docking study using (GOLD) program was performed for selected sets of the most active and inactive compounds on cyclophilin D (CypD) receptor as a major component of mPTP. Moreover, ADME profiling, *in silico* toxicity, drug-likeness, and drug-score studies were discussed. From these results, we report compound **31** as the most active nonpeptidyl mPTP blocker possessing quinazoline-urea scaffold; 2 folds of CsA activity, which would constitute a new direction for the design of novel mPTP modulators.

1. Introduction

Dementia is caused by different diseases like stroke or arteriosclerosis in the brain, traumatic brain injury, Parkinson disease and other neurodegenerative disorders. Alzheimer's disease (AD) comes to the fore as the most common cause so that it may contribute to 60–70% of cases [1–4]. Abundant evidence suggests that an important key factor associated with Alzheimer's disease etiology is the excessive production of β-amyloid peptide (Aβ) and its extracellular deposition [5]. Aβ can be found in the brains of Alzheimer's disease patients as plaques as well as small soluble oligomers [6]. Recent studies indicate that mitochondria are intracellular targets for these soluble Aβ oligomers, especially, mitochondrial permeability transition pore (mPTP) which has been reported to play a key role in mitochondrial dysfunction induced by Aβ toxicity [7,8]. The mPTP is a multiprotein complex found in the mitochondria under certain pathological conditions including oxidative stress, ischemia, strock and traumatic membrane injury [9]. It consists of three major components: a voltage-dependent anion channel (VDAC) in the outer membrane, the adenine nucleotide translocator (ANT) in the inner membrane, and cyclophilin D (CypD) in the mitochondrial matrix. In the normal state, the membrane potential is regulated by reversible opening and closing of the mPTP, which maintain intracellular calcium homeostasis. However, an accumulation of soluble Aβ oligomers in the (AD) neuronal mitochondria leads to excessive calcium entry into cytosol. The elevated calcium levels result in uncontrolled mPTP opening, inhibition of mitochondrial ATP production and severe mitochondrial swelling followed by outer membrane rupture. Hence, neuronal injury occurs due to proapoptotic proteins production from damaged mitochondria. These findings prove the role

* Corresponding author. Korea Institute of Science and Technology, Chemical Kinomics Research Center, Future Convergence Research Division, Hwarang-ro 14-gil 5, Seongbuk-gu, Seoul 136-791, South Korea.
E-mail addresses: jennyej105@hotmail.com, r8636@kist.re.kr (E.J. Roh).

http://dx.doi.org/10.1016/j.ejmech.2014.07.027
0223-5234/

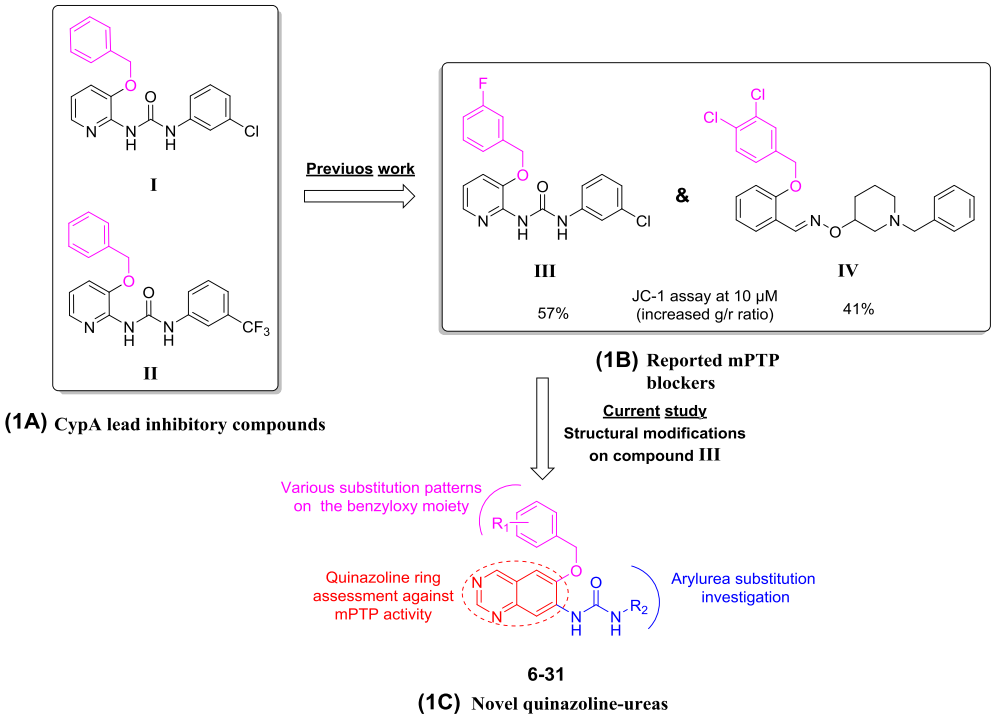

Fig. 1. Design of the quinazoline-urea derivatives **6**–**31**.

of mitochondrial dysfunction in Alzheimer's disease and lead to develop a new direction of drug targeting against neuronal mPTP which may be a promising therapeutic approach for treatment of Alzheimer's disease [7,10].

Although some peptidic compounds including Cyclosporin A (CsA) and its analogue (*N*-methyl-4-isoleucin cyclosporin (NIM811)) have been identified as mPTP inhibitors [7,11,12], they are not useful as therapeutic agents because of their poor bioavailability characteristics in addition to the hurdles of peptide delivery to the brain. Up to now, no safe mPTP inhibitors specific to the brain have been reported for AD treatment in humans [10]. Thus, the main objective of the present study was to design and synthesize novel nonpeptidyl small molecules that could inhibit the activity of the mPTP. Herein, a novel series of twenty-six quinazoline-urea analogues was designed, synthesized and biologically screened against Aβ-induced mPTP opening activity.

Since CypD is one of the three major components of mPTP protein complex, our rational design based on its high structural similarity with cyclophilin A (CypA) because these are two members of family highly homologous peptidyl prolyl *cis-trans* isomerases (PPIases) [13]. In literature, compounds **I** and **II** (Fig. 1A) were discovered as CypA inhibitory lead compounds. The common structural features of these compounds are the urea linker and 3-benzyloxyaryl moiety which are responsible for the activity [14]. Recently from our institute, two papers on compounds **III** & **IV** (Fig. 1B), supported the role of the benzyloxyaryl moiety for the activity against mPTP opening [15,16]. Accordingly, to identify novel mPTP blockers with improved *in vitro* efficacy, structural modifications were carried out on compound **III** as shown in Fig. 1C. Quinazoline core replaced the pyridine to investigate the quinazoline-urea as a new scaffold against mPTP opening activity. Variations of substitution patterns were performed on the benzyloxy moiety to evaluate the structure activity relationship. Moreover, the size of the aryl segment attached to the urea linker has been assessed through different substitutions of aryl groups.

2. Results and discussion

2.1. Chemistry

The target quinazoline-urea derivatives **6**–**31** were prepared according to the sequence of reactions depicted in Scheme 1. Heating 2,4-dinitrophenol **1** with appropriate benzylbromide in the presence of anhydrous K_2CO_3 and catalytic amount of potassium iodide in acetonitrile afforded the corresponding dinitrobenzene derivatives **2a**–**2f** which by catalytic hydrogenation at room temperature using 10% Pt/C in methanol gave the diamine analogues **3a**–**3f**. The dicarbamate derivatives **4a**–**4f** were obtained by stirring compounds **3a**–**3f** with ethyl chloroformate in the presence of triethylamine (TEA) in tetrahydrofuran (THF) at room temperature. Cyclization to quinazolineamines **5a**–**5f** was carried out by treatment of intermediates **4a**–**4f** with hexamethylenetetramine (HMTA) in the presence of trifluoroacetic acid (TFA) at room temperature, and subsequent heating with 10% aqueous-ethanolic KOH (1:1) and $K_3Fe(CN)_6$ [17]. Reaction of the amino groups in compounds **5a**–**5f** with appropriate isocyanate derivatives in THF at 85 °C provided the target quinazoline-urea derivatives **6**–**31**.

2.2. Biological evaluation

2.2.1. JC-1 assay (in vitro screening)

The ability of the new quinazoline-urea derivatives to inhibit the mitochondrial membrane potential loss is summarized in Table 1. Their activity to block the Aβ-induced mPTP opening was evaluated at a single dose concentration of 5 μM using a cell-based JC-1 assay by measuring the change of mitochondrial membrane potential [18,19]. The color shift from green to red as the membrane potential increases indicates the recovery of mitochondrial function responding to applied Aβ toxicity. In fact, compounds **III** & **IV** exhibited 57% and 41% of increased green to red ratio, respectively,

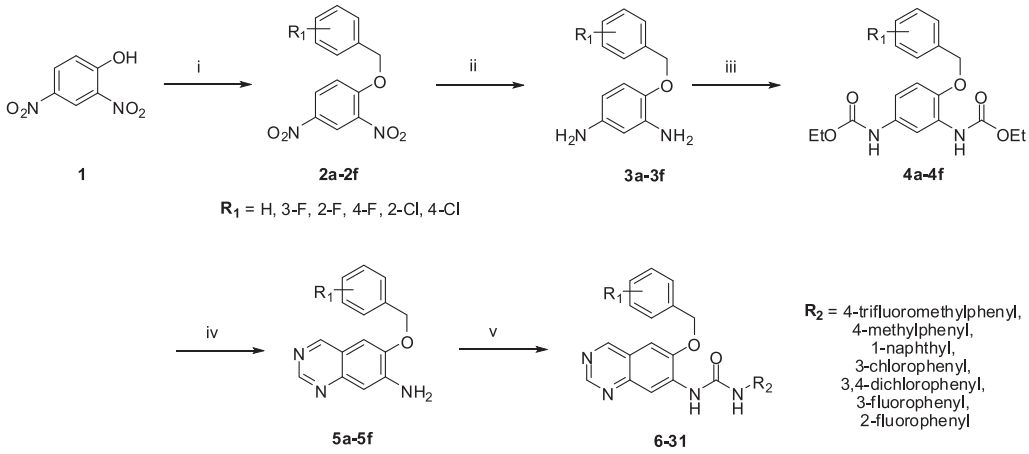

Scheme 1. Synthetic pathway of the target compounds **6**–**31**. Reagents and conditions: (i) appropriate benzylbromide, K_2CO_3, KI, CH_3CN, 75 °C, 8 h; (ii) H_2, 10% Pt/C, CH_3OH, rt, 6 h; (iii) ethyl chloroformate, TEA, THF, rt, 2 h; (iv) (a) HMTA, TFA, rt, 1 h, (b) 10% KOH aqueous ethanolic (1:1), $K_3Fe(CN)_6$, 100 °C, 4 h; (v) appropriate isocyanate derivative, THF, 85 °C, overnight.

Table 1
In vitro blocking activity of quinazoline-urea derivatives **6**–**31** against Aβ-induced mPTP opening (JC-1 assay) at single dose concentration of 5 μM.

Compd	R_1	R_2	Increased g/r ratio (%)[a]	Compd	R_1	R_2	Increased g/r ratio (%)[a]
6	H	4-Methylphenyl	154	**20**	4-F	3,4-Dichlorophenyl	155
7	H	1-Naphthyl	76	**21**	4-F	3-Fluorophenyl	61.5
8	H	3,4-Dichlorophenyl	73	**22**	4-F	2-Fluorophenyl	80.3
9	H	3-Fluorophenyl	38	**23**	2-Cl	4-Trifluoromethylphenyl	NA[b]
10	3-F	4-Methylphenyl	81	**24**	2-Cl	4-Methylphenyl	54.7
11	3-F	3-Fluorophenyl	27	**25**	2-Cl	2-Fluorophenyl	31
12	2-F	4-Trifluoromethylphenyl	68.6	**26**	4-Cl	4-Trifluoromethylphenyl	48
13	2-F	4-Methylphenyl	26.7	**27**	4-Cl	4-Methylphenyl	63
14	2-F	1-Naphthyl	39.4	**28**	4-Cl	3-Chlorophenyl	64
15	2-F	3-Chlorophenyl	51.4	**29**	4-Cl	3,4-Dichlorophenyl	91
16	2-F	3-Fluorophenyl	56.9	**30**	4-Cl	3-Fluorophenyl	29
17	4-F	4-Trifluoromethylphenyl	81	**31**	4-Cl	2-Fluorophenyl	24
18	4-F	4-Methylphenyl	99.2	**CsA**	–	–	46
19	4-F	3-Chlorophenyl	67.9				

[a] % Increase of fluorescence-ratio (green/red) after treatment of each compound and Aβ with regard to that of Aβ alone (100%). See the text for more detailed information.
[b] NA, not applicable.

which means that they were able to reduce 43% and 59% of Aβ-induced mitochondrial damage [15,16]. CsA was used as a positive standard; it exerted 46% of increased green to red ratio.

It was noted that when R_2 was 2-fluorophenyl as in **25** and **31**, or 3-fluorophenyl as in **9**, **11**, **16**, and **30**, they exhibited better inhibitory activities than those with 1-naphtyl (**7**), 4-trifluoromethylphenyl (**12**, **17**) or 4-methylphenyl (**10**, **18**). It can be deduced that the relatively bulky substituents linked to urea moiety are not well tolerated at the target site, whereas it is more favorable for the ligand to have R_2 as phenyl group substituted with small size halogen. However, compounds **13** and **14** possessing bulky substituents showed good inhibitory activities.

Of particular significance was the observation that compounds having R_1 as *para*-chlorobenzyloxy groups **26**–**31** showed improved activities than their corresponding analogues with *para*-fluorobenzyloxy groups **17**–**22**. These results could suggest that the size of the halogen groups on the benzyloxy moiety is critical for activity.

The pharmacological results indicated that seven compounds including **9**, **11**, **13**, **14**, **25**, **30** and **31** exhibited mPTP opening inhibitory activity superior to that of CsA. They revealed 38, 27, 26.7, 39.4, 31, 29, and 24% of increased green to red ratio, respectively. Compound **31** possessing *para*-chlorobenzyloxy moiety and 3-fluorophenyl segment attached to the urea linker was the most active compound in this series.

2.2.2. MTT assay (cell viability screening)

Since it is essential for the active compounds to modulate the activity of mPTP opening without exhibiting toxic effects on the cellular viability, the most active compounds were selected to measure their toxicity on the cellular activity by MTT assay at a single dose of 5 μM. As shown in Table 2, all the tested compounds revealed promising values ranging from 83 to 131%. In this event, compound **31** exerted excellent cell survival (102%), while cellular viability of 90% was achieved by the standard CsA.

2.2.3. Molecular docking

To explain the difference in inhibitory activity of the target compounds, Genetic Optimization for Ligand Docking (GOLD) [20] was used as flexible docking program to predict the different molecular binding modes of CypD with compound **III** as well as selected sets of the most active and inactive compounds based upon X-ray cocrystal structure of CypD receptor with its inhibitor CsA (PDB: 2Z6W) [21]. In CypD–CsA complex; Residues of five amino acids (Trp121, Arg55, Gln63, Asn102, and Gly72) are involved in H-bond interactions. As shown in Fig. 2; prediction showed that Compound **III** may bind to the active site through two H-bond interactions with Gln63 and Asn102 amino acid residues, in addition to a relatively weak π–π stacking interaction formed with Phe113 phenyl moiety. The current default fitness scoring function in Gold Suite-5.2 (CHEMPLP score) was used in the present study since

Table 2
MTT-cell viability assay of the most active compounds at single dose concentration of 5 μM.

Compd	MTT-cell viability (%)	Compd	MTT-cell viability (%)
9	100	**25**	101
11	104	**30**	100
13	131	**31**	102
14	83	**CsA**	90

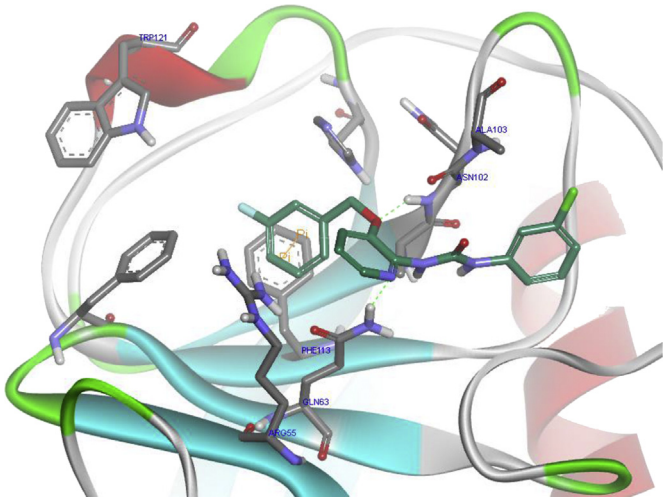

Fig. 2. Docking of compound **III** in the binding site of CypD (PDB ID: 2Z6W) in 3D style.

recent validation tests have shown it to be generally more effective than the other scoring functions for both pose prediction and virtual screening [20]. In this event, Compound **III** exerted CHEMPLP score of 61.8714.

We then clarified the different binding modes of CypD with selected sets of the most active and inactive analogues, exploiting docking calculations and CHEMPLP fitness scoring functions to get an explanation for the *in vitro* results of JC-1 assay against mPTP opening activity. The docking results showed that two possible binding modes may be energetically favored for CypD with the active set including compounds **9**, **11**, **25**, **30**, and **31**. The active ligands achieved effectively two to four H-bond interactions with CypD which led to remarkably increase of CHEMPLP scores ranging from 62.0435 to 68.9412 as listed in Table 3.

As representative hypothetical model for the first binding mode, docking of compound **25** is presented in Fig. 3. It was noted that the

Table 3
CHEMPLP scores of the docked compounds and residues of CypD involved in H-bond interactions.

Compd	CHEMPLP score	Residues of CypD involved in H-bond interactions
III	61.8714	Gln63, Asn102
9	62.0435	Gln63, Asn102, Gln111
11	65.9634	Asn102, Gln111
17	58.4236	Gln63
18	57.3575	–
20	54.8588	Asn102
22	58.1966	–
25	68.9412	Asn102, Gly109, Gln111
29	58.8383	–
30	64.2931	Gln63, Gln111
31	65.5608	Arg55, Gln63

–: No residue involved in H-bond interaction.

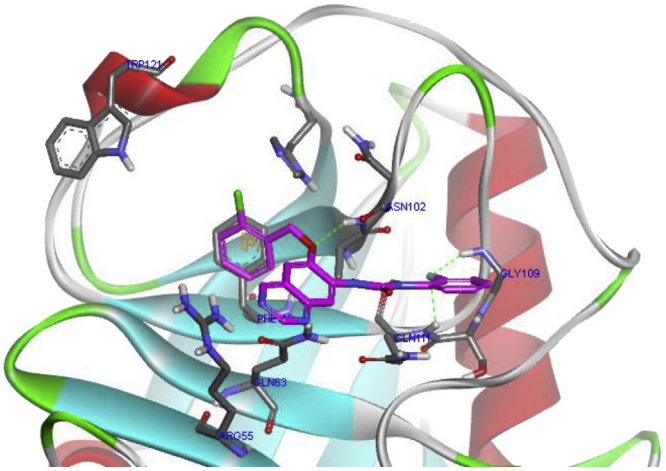

Fig. 3. Docking of compound **25** in the binding site of CypD (PDB ID: 2Z6W) in 3D style.

quinazoline-urea scaffold paved the way for the ligand to interfere more efficiently with the active site so that three H-bonds were formed with Asn102, Gly109 and Gln111 residues, in addition to stronger π–π stacking interaction with Phe113 phenyl moiety. This well-established interaction revealed high CHEMPLP score (68.94120). The second binding mode presented by compound **31**, was characterized by a ligand rotation in the active site where the benzyloxy moiety changed its position with the phenyl urea segment, however, this orientation kept three H-bond interactions with Arg55 and Gln63 residues through the urea linker as shown in Fig. 4 with high CHEMPLP score (65.5608).

On the other hand, most binding modes obtained for CypD with the inactive set including compounds **17**, **18**, **20**, **22**, and **29** clearly suggested an energetically unfavorable binding orientation characterized by perpendicular flipping of the ligand out of the binding site. Compounds **18**, **22**, and **29** couldn't establish any H-bond interaction with the target protein while both of compounds **17** and **20** achieved H-bonds with only one amino acid residue as listed in Table 3. This inefficient binding orientation resulted in relatively low CHEMPLP fitness scores ranging from 54.8588 to 58.4236. That could potentially be attributed to steric hindrance factors of the substituted groups on the phenyl urea ring. Docking models of compounds **17**, **18** and **29** possessing 4-trifluoromethylphenyl, 4-

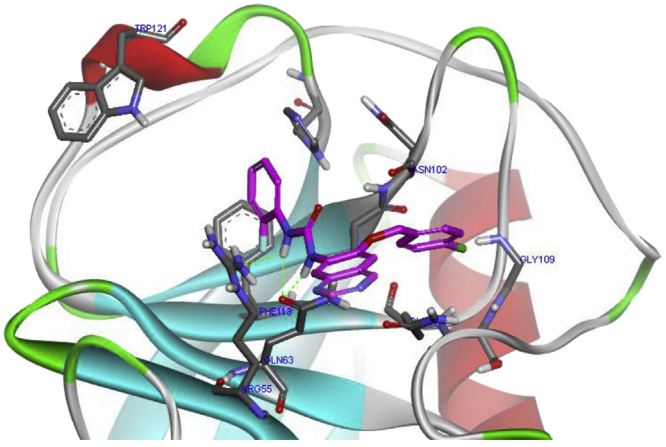

Fig. 4. Docking of compound **31** in the binding site of CypD (PDB ID: 2Z6W) in 3D style.

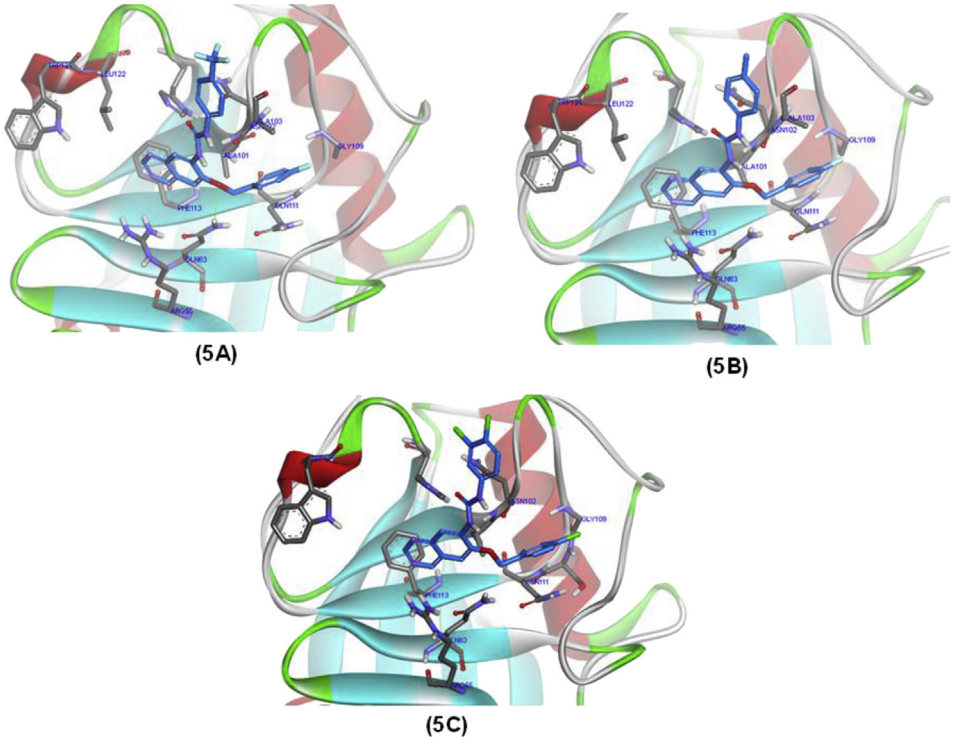

Fig. 5. Docking of compounds **17** (5A), **18** (5B), **19** (5C) in the binding site of CypD (PDB ID: 2Z6W) in 3D style.

methylphenyl, and 3,4-dichlorophenyl moieties are presented in Fig. 5.

Results of these docking study show a great variability of binding modes which may provide a possible explanation for the *in vitro* results previously discussed for JC-1 assay; compounds bearing R_2 as small halogen **9**, **11**, **25**, **30**, and **31** fitted well in the active site of CypD with high CHEMPLP scores *vice versa* compounds **17** and **18** with bulky substituents. In addition, Compounds **29**–**31** possessing *para*-chlorobenzyloxy groups showed better CHEMPLP fitness scores than those with *para*-fluorobenzyloxy groups (**17**, **18**, **20**, and **22**). Therefore, it is worth emphasizing that the relation between mPTP blocking activity and CHEMPLP scoring function was highly correlated as illustrated in Table 4.

2.2.4. Molar refractivity, total polar surface area, and ADME profiling

Since the size of the different substituents played a major role in the activity and the docking fitness scores, we investigated the influence of the molar refractometry (MR, steric factor) on the activity for the compounds with the most active analogues as listed in Table 5. Generally, it was noted that compounds **11**, **25**, **30**, and **31** with low MR values exerted higher activities against mPTP opening comparing to that of compound **14** with the highest MR value. Moreover, In case of compounds **13** and **14** with the same 2-fluorobenzyloxy moiety, the MR value of **13** possessing 4-methylphenyl segment was lower than **14** with 1-naphtylphenyl moiety *vice versa* the potency. From these results, we can conclude that MR and bulkiness are inversely proportional to the activity.

In this present report, the total polar surface area (TPSA) was also calculated since it is a key property that has been linked to drug bioavailability. Thus, passively absorbed molecules with a TPSA >140 are thought to have low oral bioavailability [22]. All the

Table 4
Correlation between the JC-1 assay *in vitro* activity and docking CHEMPLP scoring function.

Compd	JC-1 assay *in vitro* activity (increased g/r ratio (%))	CHEMPLP score	Activity
9	+	+	Active
11	+	+	Active
17	−	−	Inactive
18	−	−	Inactive
20	−	−	Inactive
22	−	−	Inactive
25	+	+	Active
29	−	−	Inactive
30	+	+	Active
31	+	+	Active

+: increased g/r ratio (%) < 40, CHEMPLP score > 62.
−: increased g/r ratio (%) > 80, CHEMPLP score < 59.

Table 5
Molar refractometry, Total polar surface area, and calculated Lipinski's rule of five for target compounds with the highest increased g/r ratio.

Comp. no.	MR[a]	Parameter						
		cLog P[b]	TPSA[c]	nHBA[d]	nHBD[e]	M.wt[f]	RB[g]	nVio[h]
9	107.67	3.96	76.14	6	2	388.39	5	0
11	108.07	4.02	76.14	6	2	406.38	5	0
13	114.17	4.72	76.14	6	2	402.42	6	1
14	124.84	5.14	76.14	6	2	438.45	5	1
25	112.27	4.57	76.14	6	2	422.84	5	1
30	112.27	4.57	76.14	6	2	422.84	5	1
31	112.27	4.57	76.14	6	2	422.84	5	1

[a] Molecular refractometry (cm^3/mol).
[b] Calculated lipophilicity.
[c] Total polar surface area ($Å^2$).
[d] Number of hydrogen bond acceptors.
[e] Number of hydrogen bond donors.
[f] Molecular weight.
[g] Rotatable bonds.
[h] Number of violations to Lipinski's rule of five.

Table 6
In silico toxicity risks and drug-likeness of target compounds with the highest increased g/r ratio comparing to lead compounds I, II and III.

Comp. no.	Drug-likeness	Toxicity effects			
		Mutagenic	Tumorigenic	Irritant	Reproductive
9	−7.42	L	L	L	M
11	−2.27	L	L	L	L
13	−1.84	M	L	L	L
14	−1.11	M	H	L	L
25	−0.01	L	L	L	L
30	0.20	L	L	L	M
31	0.32	L	L	L	M
I	−4.08	L	L	L	L
II	−4.55	L	L	L	L
III	−1.48	L	L	L	M

L: Low, M: Medium, H: High.

evaluated compounds have TPSA = 76.14 $Å^2$ (Table 5) suggesting that they have a possible good passive oral absorption.

Approximately 40% of drug candidates fail in clinical trials due to their poor ADME (absorption, distribution, metabolism, and elimination), we assessed the compliance of the most active compounds to the Lipinski rule of five [23]. Violation of more than one of these rules may result in bioavailability problems. Predictions of ADME properties using Osiris program [24] are given in Table 5. The results showed that all the studied compounds comply with these rules, consequently, good ADME properties are theoretically guaranteed.

2.2.5. In silico toxicity, drug-likeness, and drug score

Osiris program was used for prediction of the overall toxicity of the most active derivatives as the prediction process relies on a predetermined set of structural fragments that give rise to toxicity alerts in case they are encountered in the structure. Interestingly, all compounds presented low *in silico* possible toxicity risks in most cases as shown in Table 6, only except compound **14** with the bulky naphthyl moiety, showed a high risk of possible tumorigenic toxicity. These theoretical data suggest that the safety of analogues bearing small size halogen or methyl on the phenyl ring attached to the urea linker is better than the corresponding derivatives bearing bulky naphthyl group.

Currently, there are many approaches to assess a compound drug-likeness based on topological descriptors, fingerprints of molecular drug-likeness structure keys or other properties such as clog P and molecular weight [25]. In this work, Osiris program was also used for calculating the fragment-based drug-likeness of the most active compounds as illustrated in Table 6. Compounds **30** and **31** showed improvement of drug-likeness values comparing to other derivatives and lead compounds **I**, **II**, and **III**. Herein, compound **31** demonstrated the highest drug-likeness value.

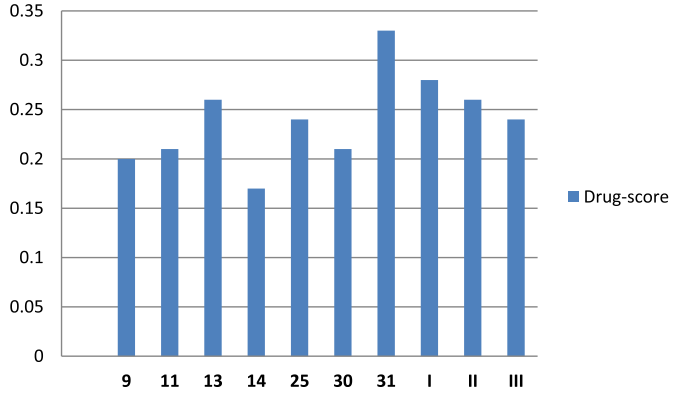

Fig. 6. *In silico* drug-score of target compounds with the highest increased g/r ratios comparing to lead compounds **I**, **II** and **III**.

Of special interest, the drug-scores of the active compounds have also been determined in the present study as shown in Fig. 6. The results showed that compound **31** exerted the highest value comparing to all series derivatives as well as all lead compounds. The *in silico* toxicity profiles, drug-likeness, and drug-score data of compound **31** make it a promising lead for future development of safe and efficient mPTP opening inhibitors.

3. Conclusion

Based on this study, we report compound **31** as the most active nonpeptidyl mPTP blocker possessing quinazoline-urea scaffold; 2 folds of CsA activity, which would constitute a new direction for the design of novel mPTP modulators as recent therapeutic approach for the treatment of Alzheimer's disease. Extensive SAR (structure–activity relationship) study as well as detailed pharmacological profile for the active analogues with *in vivo* study on Alzheimer's disease animal model will be our next plan.

4. Experimental

4.1. Chemistry

All reactions and manipulations were performed in nitrogen atmosphere using standard Schelenk techniques. Reagents and solvents were purchased from Aldrich Co. and Tokyo Chemical Industry Co. and used without purification. Thin-layer chromatography was performed with Merk silica gel 60 F_{254} pre-coated glass sheets. Column chromatography was performed on Merck Silica Gel 60 (230–400 mesh) and the eluting solvents are noted as mixed solvent with given volume-to-volume ratios. NMR (400 MHz for ^1H and 100 MHz for ^{13}C) was measured on Bruker Avance 400, and chemical shifts and coupling constants are presented in parts per million relative to Me_4Si and hertz, respectively. Abbreviations are as follows: s, singlet; d, doublet; t, triplet; q, quartet; m, multiplet; br, broad. Low-resolution spectra were carried out on Agilent 1200 Series–API 3200 LC/MS/MS System. High-resolution spectra were performed on Waters ACQUITY UPLC BEH C18 1.7μ–Q-TOF SYNAPT G2-Si High Definition Mass Spectrometry.

*4.1.1. General procedure for preparation of compounds **2a–2f***

To a solution of 2,4-dinitrophenol (0.92 g, 5 mmol) in acetonitrile (15 mL), anhydrous K_2CO_3 (2.07 g, 15 mmol) was added. The mixture was stirred for 30 min at room temperature. Catalytic amount of potassium iodide (0.17 g, 1 mmol) and the appropriate benzylbromide (5 mmol) were added. The reaction was stirred at 75 °C for 8 h. Water (125 mL) was added to the reaction mixture and the organics were extracted with ethyl acetate (3 × 125 mL). The organic layer extracts were washed with brine and dried over anhydrous Na_2SO_4. The solvent was evaporated under reduced pressure and the residue was purified by flash column chromatography (silica gel, hexane/ethyl acetate 3:1 v/v).

*4.1.1.1. 1-(Benzyloxy)-2,4-dinitrobenzene (**2a**).* Yield 58%; ^1H NMR (400 MHz, Acetone-d_6) δ [ppm]: 8.75 (d, J = 2.8 Hz, 1H), 8.52 (dd, J = 9.3, 2.8 Hz, 1H), 7.71 (d, J = 9.3 Hz, 1H), 7.54 (d, J = 8.4 Hz, 2H), 7.45–7.38 (m, 3H), 5.53 (s, 2H).

*4.1.1.2. 1-(3-Fluorobenzyloxy)-2,4-dinitrobenzene (**2b**).* Yield 70%; ^1H NMR (400 MHz, $CDCl_3$) δ [ppm]: 8.80 (d, J = 2.7 Hz, 1H), 8.43 (dd, J = 9.2, 2.7 Hz, 1H), 7.42 (dd, J = 13.6, 7.8 Hz, 1H), 7.25 (d, J = 9.2 Hz, 2H), 7.20 (d, J = 9.2 Hz, 1H), 7.10 (td, J = 8.2, 1.9 Hz, 1H), 5.38 (s, 2H).

*4.1.1.3. 1-(2-Fluorobenzyloxy)-2,4-dinitrobenzene (**2c**).* Yield 75%; ^{1}H NMR (400 MHz, DMSO-d_6) δ [ppm]: 8.79 (d, J = 2.6 Hz, 1H), 8.56 (dd, J = 9.3, 2.6 Hz, 1H), 7.78 (d, J = 9.3 Hz, 1H), 7.61 (t, J = 7.3 Hz, 1H), 7.49 (dd, J = 13.4, 6.36 Hz, 1H), 7.30 (dd, J = 11.7, 5.1 Hz, 2H), 5.54 (s, 2H). ^{13}C NMR (100 MHz, DMSO-d_6) δ 161.99, 159.54, 155.76, 140.43, 139.25, 131.51, 130.88, 129.81, 125.16, 122.52, 121.72, 116.52, 66.70.

*4.1.1.4. 1-(4-Fluorobenzyloxy)-2,4-dinitrobenzene (**2d**).* Yield 68%; ^{1}H NMR (400 MHz, $CDCl_3$) δ [ppm]: 8.79 (d, J = 2.7 Hz, 1H), 8.44 (dd, J = 9.2, 2.7 Hz, 1H), 7.47 (dd, J = 8.3, 5.2 Hz, 2H), 7.26 (s, 1H), 7.14 (t, J = 8.6 Hz, 2H), 5.35 (s, 2H).

*4.1.1.5. 1-(2-Chlorobenzyloxy)-2,4-dinitrobenzene (**2e**).* Yield 75%; ^{1}H NMR (400 MHz, DMSO-d_6) δ [ppm]: 8.80 (d, J = 2.6 Hz, 1H), 8.55 (dd, J = 9.2, 2.6 Hz, 1H), 7.75 (d, J = 9.2 Hz, 1H), 7.64 (t, J = 4.0 Hz, 1H), 7.55 (t, J = 4.0 Hz, 1H), 7.45–7.43 (m, 2H), 5.55 (s, 2H).

*4.1.1.6. 1-(4-Chlorobenzyloxy)-2,4-dinitrobenzene (**2f**).* Yield 62%; ^{1}H NMR (400 MHz, Acetone-d_6) δ [ppm]: 8.75 (d, J = 2.8 Hz, 1H), 8.52 (dd, J = 9.3, 2.8 Hz, 1H), 7.69 (d, J = 9.3 Hz, 1H), 7.55 (d, J = 8.4 Hz, 2H), 7.45 (d, J = 8.4 Hz, 2H), 5.53 (s, 2H). ^{13}C NMR (100 MHz, Acetone-d_6) δ [ppm]: 156.83, 141.33, 140.21, 135.07, 134.73, 130.17, 130.10, 129.84, 129.66, 129.59, 122.21, 116.65, 72.03.

*4.1.2. General procedure for preparation of compounds **3a**–**3f***

To a solution of compound **2a**–**2f** (4.2 mmol) in methanol (70 mL), 10% Pt/C (0.42 mmol) was added and the reaction mixture was stirred under hydrogen atmosphere at room temperature for 6 h. The mixture was filtered through celite and the filtrate was evaporated under reduced pressure and the residue was purified by flash column chromatography (silica gel, hexane/ethyl acetate 1:1 v/v) to afford the desired diamines.

*4.1.2.1. 4-(Benzyloxy)benzene-1,3-diamine (**3a**).* Yield 85%; ^{1}H NMR (400 MHz, $CDCl_3$) δ [ppm]: 7.46–7.34 (m, 5H), 6.71 (d, J = 8.4 Hz, 1H), 6.17 (d, J = 2.6 Hz, 1H), 6.06 (dd, J = 8.4, 2.6 Hz, 1H), 5.01 (s, 2H).

*4.1.2.2. 4-(3-Fluorobenzyloxy)benzene-1,3-diamine (**3b**).* Yield 88%; ^{1}H NMR (400 MHz, $CDCl_3$) δ [ppm]: 7.33 (dd, J = 13.0, 7.5 Hz, 1H), 7.17 (dd, J = 13.0, 7.5 Hz, 2H), 7.01 (t, J = 8.4 Hz, 1H), 6.65 (d, J = 8.4 Hz, 1H), 6.14 (d, J = 2.0 Hz, 1H), 6.03 (dd, J = 8.4, 2.0 Hz, 1H), 4.98 (s, 2H).

*4.1.2.3. 4-(2-Fluorobenzyloxy)benzene-1,3-diamine (**3c**).* Yield 90%; ^{1}H NMR (400 MHz, $CDCl_3$) δ [ppm]: 7.40 (t, J = 6.5 Hz, 1H), 7.21 (d, J = 6.5 Hz, 1H), 7.07–6.98 (m, 2H), 6.63 (d, J = 8.7 Hz, 1H), 5.9 (s, 2H), 4.95 (s, 2H), 3.76 (s, 2H), 3.35 (s, 2H). ^{13}C NMR (100 MHz, $CDCl_3$) δ [ppm]: 161.85, 141.84, 139.55, 138.10, 130.20, 129.86, 124.86, 124.30, 115.41, 115.15, 104.93, 103.60, 67.12.

*4.1.2.4. 4-(4-Fluorobenzyloxy)benzene-1,3-diamine (**3d**).* Yield 92%; ^{1}H NMR (400 MHz, $CDCl_3$) δ [ppm]: 7.41 (dd, J = 8.5, 5.5 Hz, 2H), 7.08 (t, J = 8.5 Hz, 2H), 6.68 (d, J = 8.5 Hz, 1H), 6.17 (d, J = 2.5 Hz, 1H), 6.07 (dd, J = 8.5, 2.5 Hz, 1H), 4.96 (s, 2H).

*4.1.2.5. 4-(2-Chlorobenzyloxy)benzene-1,3-diamine (**3e**).* Yield 95%; ^{1}H NMR (400 MHz, DMSO-d_6) δ [ppm]: 7.65–7.63 (m, 1H), 7.50–7.47 (m, 1H), 7.39–7.36 (m, 2H), 6.57 (d, J = 8.3 Hz, 1H), 5.97 (d, J = 2.3 Hz, 1H), 5.75 (dd, J = 8.3, 2.3 Hz, 1H), 4.95 (s, 2H), 4.53 (s, 2H), 4.42 (s, 2H).

*4.1.2.6. 4-(4-Chlorobenzyloxy)benzene-1,3-diamine (**3f**).* Yield 75%; ^{1}H NMR (400 MHz, $CDCl_3$) δ [ppm]: 7.37 (br, 2H), 7.36 (br, 2H), 7.34–7.29 (m, 3H), 4.70 (s, 2H).

*4.1.3. General procedure for preparation of compounds **4a**–**4f***

A mixture of diamine **3a**–**3f** (4 mmol), ethyl chloroformate (16 mmol), and TEA (16 mmol) in anhydrous THF (40 mL) was stirred at room temperature for 2 h. The solid was filtered off and the solution was evaporated under reduced pressure. The residue was dissolved in EtOAc (100 mL) and the organic phase was washed with water (2 × 100 mL). The organic phase was evaporated under reduced pressure and the residue was purified by flash column chromatography (silica gel, hexane/ethyl acetate 4:1 v/v) to yield the corresponding dicarbamates **4a**–**4f**.

*4.1.3.1. Diethyl 4-(benzyloxy)-1,3-phenylenedicarbamate (**4a**).* Yield 86%; ^{1}H NMR (400 MHz, Acetone-d_6) δ [ppm]: 8.46 (s, 1H), 8.28 (d, J = 2.5 Hz, 1H), 7.59 (s, 1H), 7.49 (d, J = 8.3 Hz, 2H), 7.42–7.34 (m, 4H), 6.99 (d, J = 8.9 Hz, 1H), 5.12 (s, 2H), 4.17 (q, J = 7.1 Hz, 4H), 1.25 (t, J = 7.1 Hz, 6H). ^{13}C NMR (100 MHz, $CDCl_3$) δ [ppm]: 153.93, 153.27, 143.15, 137.09, 132.99, 128.53, 128.35, 127.90, 113.14, 112.39, 110.38, 70.86, 60.75, 14.07.

*4.1.3.2. Diethyl 4-(3-fluorobenzyloxy)-1,3-phenylenedicarbamate (**4b**).* Yield 83%; ^{1}H NMR (400 MHz, $CDCl_3$) δ [ppm]: 7.99 (s, 1H), 7.38 (dd, J = 13.2, 7.4 Hz, 1H), 7.18 (d, J = 8.3 Hz, 2H), 7.13 (d, J = 8.4 Hz, 1H), 7.07 (t, J = 8.6 Hz, 1H), 6.84 (d, J = 8.9 Hz, 1H), 6.23 (s, 1H), 5.09 (s, 2H), 4.24 (q, J = 7.0 Hz, 4H), 1.33 (t, J = 7.0 Hz, 6H). HRMS (ES+): m/z calculated for $C_{19}H_{21}FN_2O_5$: 399.1332 $[M+Na]^+$. Found 399.1326.

*4.1.3.3. Diethyl 4-(2-fluorobenzyloxy)-1,3-phenylenedicarbamate (**4c**).* Yield 70%; ^{1}H NMR (400 MHz, $CDCl_3$) δ [ppm]: 8.07 (s, 1H), 7.38–7.28 (m, 3H), 7.13–7.04 (m, 2H), 6.85 (d, J = 8.4 Hz, 1H), 5.07 (s, 2H), 4.17 (q, J = 6.5 Hz, 4H), 1.25 (t, J = 6.5 Hz, 6H). ^{13}C NMR (100 MHz, $CDCl_3$) δ [ppm]: 158.75, 152.03, 151.48, 140.55, 130.57, 128.73, 128.21, 125.61, 122.28, 121.60, 113.56, 111.07, 110.47, 107.92, 63.28, 60.23, 12.53.

*4.1.3.4. Diethyl 4-(4-fluorobenzyloxy)-1,3-phenylenedicarbamate (**4d**).* Yield 80%; ^{1}H NMR (400 MHz, $CDCl_3$) δ [ppm]: 7.99 (d, J = 2.2 Hz, 1H), 7.39 (dd, J = 8.7, 5.4 Hz, 2H), 7.18 (s, 1H), 7.11 (t, J = 8.7 Hz, 2H), 6.87 (d, J = 8.7 Hz, 1H), 6.58 (s, 1H), 5.05 (s, 2H), 4.23 (q, J = 7.0 Hz, 4H), 1.32 (t, J = 7.0 Hz, 6H). HRMS (ES$^+$): m/z calculated for $C_{19}H_{21}FN_2O_5$: 399.1332 $[M+Na]^+$. Found 399.1328.

*4.1.3.5. Diethyl 4-(2-chlorobenzyloxy)-1,3-phenylenedicarbamate (**4e**).* Yield 88%; ^{1}H NMR (400 MHz, DMSO-d_6) δ [ppm]: 9.46 (s, 1H), 8.32 (s, 1H), 7.79 (s, 1H), 7.65 (s, 1H), 7.52–7.50 (m, 1H), 7.40–7.38 (m, 2H), 7.14 (d, J = 7.7 Hz, 1H), 7.01 (d, J = 8.9 Hz, 1H), 5.15 (s, 2H), 4.06 (q, J = 6.3 Hz, 4H), 1.22 (t, J = 6.3 Hz, 6H).

*4.1.3.6. Diethyl 4-(4-chlorobenzyloxy)-1,3-phenylenedicarbamate (**4f**).* Yield 88%; ^{1}H NMR (400 MHz, Acetone-d_6) δ [ppm]: 8.46 (s, 1H), 8.18 (d, J = 2.4 Hz, 1H), 7.60 (s, 1H), 7.54 (d, J = 8.5 Hz, 2H), 7.44 (d, J = 8.5 Hz, 2H), 7.28 (d, J = 7.2 Hz, 1H), 7.01 (d, J = 8.9 Hz, 1H), 5.17 (s, 2H), 4.15 (q, J = 6.8 Hz, 4H), 1.26 (t, J = 6.8 Hz, 6H). HRMS (ES$^+$): m/z calculated for $C_{19}H_{21}ClN_2O_5$: 415.1037 $[M+Na]^+$. Found 415.1034.

*4.1.4. General procedure for preparation of compounds **5a**–**5f***

A mixture of dicarbamate **4a**–**4f** (5 mmol) and HMTA (35 mmol) in TFA (35 mL) was refluxed for 1 h. The mixture was then cooled to room temperature and diluted with 4 M HCl (200 mL). The undissolved residue was filtered off and the solution was evaporated under reduced pressure. The residue was dissolved in aqueous ethanolic (H_2O/EtOH, 1/1) 10% KOH (300 mL), added of $K_3Fe(CN)_6$ (12.5 g, 38 mmol) and refluxed for 4 h. After cooling, the mixture was diluted with water (300 mL), extracted with ethyl acetate

(500 mL), and the organic phase was evaporated under reduced pressure. The residue was purified by flash column chromatography (silica gel, methylene chloride/methanol 25:1 v/v).

*4.1.4.1. 6-(Benzyloxy)quinazolin-7-amine (**5a**).* Yield 30%; ^{1}H NMR (400 MHz, $CDCl_3$) δ [ppm]: 9.03 (s, 1H), 8.99 (s, 1H), 7.49–7.38 (m, 5H), 7.08 (d, J = 1.9 Hz, 2H), 5.25 (s, 2H), 4.75 (s, 2H). LC/MS (ESI+): *m/z* calculated for $C_{15}H_{13}N_3O$: 252.1 $[M+H]^+$. Found 252.1.

*4.1.4.2. 6-(3-Fluorobenzyloxy)quinazolin-7-amine (**5b**).* Yield 20%; ^{1}H NMR (400 MHz, $CDCl_3$) δ [ppm]: 9.03 (s, 1H), 8.98 (s, 1H), 7.39 (dd, J = 7.6, 5.8 Hz, 1H), 7.24 (s, 1H), 7.19 (d, J = 9.2 Hz, 1H), 7.09–7.04 (m, 3H), 5.24 (s, 2H), 4.75 (s, 2H).

*4.1.4.3. 6-(2-Fluorobenzyloxy)quinazolin-7-amine (**5c**).* Yield 25%; ^{1}H NMR (400 MHz, $CDCl_3$) δ [ppm]: 9.06 (s, 1H), 9.03 (s, 1H), 7.52 (t, J = 8.8 Hz, 1H), 7.42 (dd, J = 13.6, 5.9 Hz, 1H), 7.25–7.18 (m, 2H), 7.15 (s, 1H), 7.12 (s, 1H), 5.34 (s, 2H), 4.45 (s, 2H). ^{13}C NMR (100 MHz, $CDCl_3$) δ [ppm]: 163.01, 156.42, 154.22, 148.43, 147.51, 144.87, 130.62, 130.06, 124.52, 122.75, 119.62, 116.15, 106.64, 104.47, 64.73.

*4.1.4.4. 6-(4-Fluorobenzyloxy)quinazolin-7-amine (**5d**).* Yield 32%; ^{1}H NMR (400 MHz, $CDCl_3$) δ [ppm]: 9.06 (s, 1H), 9.02 (s, 1H), 7.48 (dd, J = 8.5, 5.3 Hz, 2H), 7.15 (t, J = 8.5 Hz, 2H), 7.11 (d, J = 4.6 Hz, 2H), 5.23 (s, 2H), 4.74 (s, 2H).

*4.1.4.5. 6-(2-Chlorobenzyloxy)quinazolin-7-amine (**5e**).* Yield 27%; ^{1}H NMR (400 MHz, DMSO-d_6) δ [ppm]: 9.02 (s, 1H), 8.83 (s, 1H), 7.82–7.78 (m, 1H), 7.57–7.53 (m, 1H), 7.48–7.42 (m, 3H), 6.95 (s, 1H), 6.27–6.26 (m, 2H), 5.36 (s, 2H).

*4.1.4.6. 6-(4-Chlorobenzyloxy)quinazolin-7-amine (**5f**).* Yield 37%; ^{1}H NMR (400 MHz, $CDCl_3$) δ [ppm]: 9.04 (s, 1H), 8.99 (s, 1H), 7.43 (br, 4H), 7.12 (s, 1H), 7.07 (s, 1H), 5.22 (s, 2H), 4.80 (s, 2H). ^{13}C NMR (100 MHz, $CDCl_3$) δ 156.28, 154.20, 148.39, 147.52, 144.82, 134.55, 134.09, 129.12, 119.56, 106.59, 104.47, 70.10.

*4.1.5. General procedure for preparation of compounds **6**–**31***

A mixture of quinazolinamines **5a**–**5f** (1.0 mmol) and the appropriate isocyanate derivative (1.2 mmol) in anhydrous THF (10 mL) was stirred at 85 °C overnight. The mixture was evaporated under reduced pressure and the residue was purified by flash column chromatography (silica gel, methylene chloride/ethyl acetate 1:4 v/v).

*4.1.5.1. 1-(6-(Benzyloxy)quinazolin-7-yl)-3-p-tolylurea (**6**).* Yield 64%; ^{1}H NMR (400 MHz, Acetone-d_6) δ [ppm]: 9.17 (s, 1H), 9.06 (s, 1H), 8.97 (s, 1H), 8.89 (s, 1H), 8.53 (s, 1H), 7.67–7.56 (m, 3H), 7.46–7.39 (m, 5H), 7.11 (d, J = 8.4 Hz, 2H), 5.43 (s, 2H), 2.29 (s, 3H). HRMS (ES^+): *m/z* calculated for $C_{23}H_{20}N_4O_2$: 407.1484 $[M+Na]^+$. Found 407.1493.

*4.1.5.2. 1-(6-(Benzyloxy)quinazolin-7-yl)-3-(naphthalen-1-yl)urea (**7**).* Yield 72%; ^{1}H NMR (400 MHz, DMSO-d_6) δ [ppm]: 9.78 (s, 1H), 9.30 (s, 1H), 9.26 (s, 1H), 9.06 (s, 1H), 8.80 (s, 1H), 8.21 (d, J = 8.0 Hz, 1H), 7.98 (t, J = 7.6 Hz, 2H), 7.72 (d, J = 8.0 Hz, 1H), 7.67 (s, 1H), 7.63–7.45 (m, 8H), 5.54 (s, 2H). ^{13}C NMR (100 MHz, DMSO-d_6) δ [ppm]: 162.80, 157.62, 154.30, 153.30, 147.80, 147.11, 137.70, 136.44, 134.24, 134.12, 129.15, 128.87, 128.69, 128.27, 127.14, 126.51, 126.31, 124.43, 122.41, 121.00, 119.62, 113.41, 106.14, 70.94. LC/MS (ESI+): *m/z* calculated for $C_{26}H_{20}N_4O_2$: 421.16 $[M+H]^+$. Found 421.13.

*4.1.5.3. 1-(6-(Benzyloxy)quinazolin-7-yl)-3-(3,4-dichlorophenyl)urea (**8**).* Yield 58%; ^{1}H NMR (400 MHz, DMSO-d_6) δ [ppm]: 10.09 (s, 1H), 9.26 (s, 1H), 9.08 (s, 1H), 8.86 (s, 1H), 8.73 (s, 1H), 7.96–7.93 (m, 1H), 7.67 (s, 1H), 7.60 (d, J = 7.1 Hz, 2H), 7.56 (d, J = 8.8 Hz, 1H), 7.45 (t, J = 7.1 Hz, 2H), 7.40–7.34 (m, 2H), 5.48 (s, 2H). ^{13}C NMR (100 MHz, DMSO-d_6) δ [ppm]: 162.80, 157.72, 154.39, 152.38, 147.66, 147.00, 139.81, 137.03, 136.29, 131.68, 131.26, 129.13, 128.75, 128.46, 124.28, 121.17, 120.01, 119.02, 113.41, 106.20, 71.00. LC/MS (ESI+): *m/z* calculated for $C_{22}H_{16}Cl_2N_4O_2$: 439.07 $[M+H]^+$. Found 439.06.

*4.1.5.4. 1-(6-(Benzyloxy)quinazolin-7-yl)-3-(3-fluorophenyl)urea (**9**).* Yield 40%; ^{1}H NMR (400 MHz, DMSO-d_6) δ [ppm]: 10.01 (s, 1H), 9.26 (s, 1H), 9.07 (s, 1H), 8.87 (s, 1H), 8.75 (s, 1H), 7.66 (s, 1H), 7.61–7.55 (m, 3H), 7.46 (t, J = 7.8 Hz, 2H), 7.40–7.35 (m, 2H), 7.16 (d, J = 8.1 Hz, 1H), 6.86 (t, J = 8.1 Hz, 1H), 5.49 (s, 2H). HRMS (ES^+): *m/z* calculated for $C_{22}H_{17}FN_4O_2$: 389.1414 $[M+H]^+$. Found 389.1410.

*4.1.5.5. 1-(6-(3-Fluorobenzyloxy)quinazolin-7-yl)-3-p-tolylurea (**10**).* Yield 75%; ^{1}H NMR (400 MHz, DMSO-d_6) δ [ppm]: 9.67 (s, 1H), 9.25 (s, 1H), 9.07 (s, 1H), 8.77 (d, J = 4.8 Hz, 2H), 7.65 (s, 1H), 7.51–7.40 (m, 5H), 7.22 (t, J = 7.9 Hz, 1H), 7.14 (d, J = 7.9 Hz, 2H), 5.49 (s, 2H), 2.27 (s, 3H). HRMS (ES^+): *m/z* calculated for $C_{23}H_{19}FN_4O_2$: 425.1390 $[M+Na]^+$. Found 425.1396.

*4.1.5.6. 1-(6-(3-Fluorobenzyloxy)quinazolin-7-yl)-3-(3-fluorophenyl) urea (**11**).* Yield 66%; ^{1}H NMR (400 MHz, DMSO-d_6) δ [ppm]: 9.98 (s, 1H), 9.26 (s, 1H), 9.08 (s, 1H), 8.86 (s, 1H), 8.75 (s, 1H), 7.65 (s, 1H), 7.56 (d, J = 11.6 Hz, 1H), 7.53–7.42 (m, 3H), 7.37 (dd, J = 15.4, 7.8 Hz, 1H), 7.22 (t, J = 7.8 Hz, 1H), 7.16 (d, J = 7.8 Hz, 1H), 6.85 (t, J = 7.8 Hz, 1H), 5.49 (s, 2H). HRMS (ES^+): *m/z* calculated for $C_{22}H_{16}F_2N_4O_2$: 429.1139 $[M+Na]^+$. Found 429.1143.

*4.1.5.7. 1-(6-(2-Fluorobenzyloxy)quinazolin-7-yl)-3-(4-(trifluoromethyl)phenyl)urea (**12**).* Yield 69%; ^{1}H NMR (400 MHz, DMSO-d_6) δ [ppm]: 10.17 (s, 1H), 9.31 (s, 1H), 9.09 (s, 1H), 8.84 (s, 1H), 8.77 (s, 1H), 7.76–7.69 (m, 6H), 7.50–7.48 (m, 1H), 7.36–7.30 (m, 2H), 5.50 (s, 2H). HRMS (ES^+): *m/z* calculated for $C_{23}H_{16}F_4N_4O_2$: 479.1107 $[M+Na]^+$. Found 479.1109.

*4.1.5.8. 1-(6-(2-Fluorobenzyloxy)quinazolin-7-yl)-3-p-tolylurea (**13**).* Yield 53%; ^{1}H NMR (400 MHz, MeOD) δ [ppm]: 9.19 (s, 1H), 8.99 (s, 1H), 8.87 (s, 1H), 7.64 (t, J = 7.4 Hz, 1H), 7.57 (s, 1H), 7.47 (dd, J = 12.5, 5.0 Hz, 1H), 7.32 (d, J = 8.2 Hz, 2H), 7.29–7.21 (m, 2H), 7.09 (d, J = 8.2 Hz, 2H), 5.45 (s, 2H), 2.29 (s, 3H). HRMS (ES^+): *m/z* calculated for $C_{23}H_{19}FN_4O_2$: 425.1390 $[M+Na]^+$. Found 425.1390.

*4.1.5.9. 1-(6-(2-Fluorobenzyloxy)quinazolin-7-yl)-3-(naphthalen-1-yl)urea (**14**).* Yield 33%; ^{1}H NMR (400 MHz, DMSO-d_6) δ [ppm]: 9.76 (s, 1H), 9.30 (s, 1H), 9.18 (s, 1H), 9.09 (s, 1H), 8.82 (s, 1H), 8.17 (d, J = 8.2 Hz, 1H), 7.97–7.95 (m, 2H), 7.74–7.69 (m, 3H), 7.63–7.48 (m, 4H), 7.36–7.29 (m, 2H), 5.55 (s, 2H). LC/MS (ESI+): *m/z* calculated for $C_{26}H_{19}FN_4O_2$: 439.16 $[M+H]^+$. Found 439.13.

*4.1.5.10. 1-(3-Chlorophenyl)-3-(6-(2-fluorobenzyloxy)quinazolin-7-yl)urea (**15**).* Yield 53%; ^{1}H NMR (400 MHz, DMSO-d_6) δ [ppm]: 9.98 (s, 1H), 9.30 (s, 1H), 9.09 (s, 1H), 8.75 (br, 2H), 7.76 (d, J = 9.5 Hz, 2H), 7.70 (t, J = 7.6 Hz, 1H), 7.49 (dd, J = 13.2, 5.8 Hz, 1H), 7.36–7.26 (m, 4H), 7.07 (d, J = 7.6 Hz, 1H), 5.50 (s, 2H). HRMS (ES^+): *m/z* calculated for $C_{22}H_{16}ClFN_4O_2$: 423.1024 $[M+H]^+$. Found 423.1063; 445.0844 $[M+Na]^+$. Found 445.0886.

*4.1.5.11. 1-(6-(2-Fluorobenzyloxy)quinazolin-7-yl)-3-(3-fluorophenyl)urea (**16**).* Yield 63%; ^{1}H NMR (400 MHz, DMSO-d_6) δ [ppm]: 9.99 (s, 1H), 9.30 (s, 1H), 9.09 (s, 1H), 8.18 (s, 1H), 8.76 (s, 1H), 7.75 (s, 1H), 7.70 (t, J = 7.5 Hz, 1H), 7.56–7.47 (m, 2H), 7.38–7.28 (m, 3H), 7.14 (d, J = 8.1 Hz, 1H), 6.85 (td, J = 6.3, 1.9 Hz, 1H), 5.50 (s, 2H). LC/MS (ESI+): *m/z* calculated for $C_{22}H_{16}F_2N_4O_2$: 407.13 $[M+H]^+$. Found 407.13.

*4.1.5.12. 1-(6-(4-Fluorobenzyloxy)quinazolin-7-yl)-3-(4-(trifluoromethyl)phenyl)urea (**17**).* Yield 81%; ^{1}H NMR (400 MHz, Acetone-d_6) δ [ppm]: 9.22 (br, 2H), 9.08 (s, 1H), 8.96 (s, 1H), 8.62 (s, 1H), 7.78 (d, J = 8.6 Hz, 2H), 7.70–7.63 (m, 5H), 7.23 (t, J = 8.6 Hz, 2H), 5.47 (s, 2H). HRMS (ES$^+$): *m/z* calculated for $C_{23}H_{16}F_4N_4O_2$: 457.1287 [M+H]$^+$. Found 457.1285; 479.1107 [M+Na]$^+$. Found 479.1103.

*4.1.5.13. 1-(6-(4-Fluorobenzyloxy)quinazolin-7-yl)-3-p-tolylurea (**18**).* Yield 78%; ^{1}H NMR (400 MHz, $CDCl_3$) δ [ppm]: 9.15 (s, 1H), 9.08 (s, 1H), 8.94 (s, 1H), 7.95 (s, 1H), 7.32–7.29 (m, 2H), 7.15 (d, J = 8.2 Hz, 2H), 7.10 (s, 1H), 7.05 (t, J = 8.5 Hz, 2H), 6.98 (d, J = 8.2 Hz, 2H), 5.08 (s, 2H), 2.29 (s, 3H). HRMS (ES−): *m/z* calculated for $C_{23}H_{19}FN_4O_2$: 401.1414 [M−H]$^-$. Found 401.1416.

*4.1.5.14. 1-(3-Chlorophenyl)-3-(6-(4-fluorobenzyloxy)quinazolin-7-yl)urea (**19**).* Yield 64%; ^{1}H NMR (400 MHz, Acetone-d_6) δ [ppm]: 9.21 (s, 1H), 9.11 (s, 1H), 9.08 (s, 1H), 8.95 (s, 1H), 8.60 (s, 1H), 7.83 (t, J = 2.0 Hz, 1H), 7.68 (dd, J = 8.6, 5.5 Hz, 2H), 7.63 (s, 1H), 7.39–7.30 (m, 2H), 7.23 (t, J = 8.8 Hz, 2H), 7.07 (dt, J = 7.8, 1.2 Hz, 1H), 5.47 (s, 2H). HRMS (ES$^-$): *m/z* calculated for $C_{22}H_{16}ClFN_4O_2$: 421.0868 [M−H]$^-$. Found 421.0849.

*4.1.5.15. 1-(3,4-Dichlorophenyl)-3-(6-(4-fluorobenzyloxy)quinazolin-7-yl)urea (**20**).* Yield 83%; ^{1}H NMR (400 MHz, Acetone-d_6) δ [ppm]: 9.27 (s, 1H), 9.21 (s, 1H), 9.07 (s, 1H), 8.92 (s, 1H), 8.63 (s, 1H), 7.97 (d, J = 2.3 Hz, 1H), 7.70–7.65 (m, 2H), 7.63 (s, 1H), 7.50–7.42 (m, 2H), 7.23 (t, J = 8.8 Hz, 2H), 5.47 (s, 2H). HRMS (ES$^-$): *m/z* calculated for $C_{22}H_{15}Cl_2FN_4O_2$: 455.0478 [M−H]−. Found 455.0470.

*4.1.5.16. 1-(6-(4-Fluorobenzyloxy)quinazolin-7-yl)-3-(3-fluorophenyl)urea (**21**).* Yield 66%; ^{1}H NMR (400 MHz, $CDCl_3$) δ [ppm]: 9.12 (s, 1H), 9.04 (s, 1H), 8.88 (s, 1H), 8.09 (s, 1H), 8.02 (s, 1H), 7.36 (dd, J = 8.2, 5.4 Hz, 2H), 7.19 (d, J = 10.8 Hz, 1H), 7.10–7.01 (m, 4H), 6.93 (d, J = 7.7 Hz, 1H), 6.71 (t, J = 7.7 Hz, 1H), 5.09 (s, 2H). LC/MS (ESI+): *m/z* calculated for $C_{22}H_{16}F_2N_4O_2$: 407.13 [M+H]$^+$. Found 407.13.

*4.1.5.17. 1-(6-(4-Fluorobenzyloxy)quinazolin-7-yl)-3-(2-fluorophenyl)urea (**22**).* Yield 68%; ^{1}H NMR (400 MHz, Acetone-d_6) δ [ppm]: 9.21 (s, 1H), 9.07 (s, 1H), 9.02 (s, 1H), 8.98 (s, 1H), 8.69 (s, 1H), 8.35 (td, J = 8.2, 1.6 Hz, 1H), 7.66 (dd, J = 8.5, 5.4 Hz, 2H), 7.62 (s, 1H), 7.25–7.16 (m, 4H), 7.14–7.07 (m, 1H), 5.45 (s, 2H). HRMS (ES$^+$): *m/z* calculated for $C_{22}H_{16}F_2N_4O_2$: 429.1139 [M+Na]$^+$. Found 429.1135.

*4.1.5.18. 1-(6-(2-Chlorobenzyloxy)quinazolin-7-yl)-3-(4-(trifluoromethyl)phenyl)urea (**23**).* Yield 76%; ^{1}H NMR (400 MHz, DMSO-d_6) δ [ppm]: 10.19 (s, 1H), 9.31 (s, 1H), 9.10 (s, 1H), 8.86 (s, 1H), 8.78 (s, 1H), 7.72–7.67 (m, 6H), 7.61–7.59 (m, 1H), 7.46–7.44 (m, 2H), 5.52 (s, 2H). HRMS (ES$^+$): *m/z* calculated for $C_{23}H_{16}ClF_3N_4O_2$: 473.0992 [M+H]$^+$. Found 473.0987; 495.0812 [M+Na]$^+$. Found 495.0808.

*4.1.5.19. 1-(6-(2-Chlorobenzyloxy)quinazolin-7-yl)-3-p-tolylurea (**24**).* Yield 54%; ^{1}H NMR (400 MHz, DMSO-d_6) δ [ppm]: 9.68 (s, 1H), 9.29 (s, 1H), 9.08 (s, 1H), 8.77 (s, 1H), 8.71 (s, 1H), 7.73–7.69 (m, 2H), 7.59 (d, J = 6.4 Hz, 1H), 7.46–7.44 (m, 2H), 7.38 (d, J = 7.8 Hz, 2H), 7.13 (d, J = 7.8 Hz, 2H), 5.50 (s, 2H), 2.26 (s, 3H). HRMS (ES$^+$): *m/z* calculated for $C_{23}H_{19}ClN_4O_2$: 441.1095 [M+Na]$^+$. Found 441.1095.

*4.1.5.20. 1-(6-(2-Chlorobenzyloxy)quinazolin-7-yl)-3-(2-fluorophenyl)urea (**25**).* Yield 81%; ^{1}H NMR (400 MHz, DMSO-d_6) δ [ppm]: 9.69 (s, 1H), 9.30 (s, 1H), 9.27 (s, 1H), 9.09 (s, 1H), 8.78 (s, 1H), 8.17 (td, J = 8.2, 1.4 Hz, 1H), 7.71–7.68 (m, 2H), 7.60–7.57 (m, 1H), 7.48–7.42 (m, 2H), 7.29–7.24 (m, 1H), 7.17 (t, J = 7.7 Hz, 1H), 7.10–7.07 (m, 1H), 5.52 (s, 2H). HRMS (ES$^+$): *m/z* calculated for $C_{22}H_{16}ClFN_4O_2$: 423.1024 [M+H]$^+$. Found 423.1023.

*4.1.5.21. 1-(6-(4-Chlorobenzyloxy)quinazolin-7-yl)-3-(4-(trifluoromethyl)phenyl)urea (**26**).* Yield 75%; ^{1}H NMR (400 MHz, Acetone-d_6) δ [ppm]: 9.29 (s, 1H), 9.20 (s, 1H), 9.08 (s, 1H), 8.95 (s, 1H), 8.65 (s, 1H), 7.78 (d, J = 8.0 Hz, 2H), 7.65 (dd, J = 8.5, 2.0 Hz, 4H), 7.61 (s, 1H), 7.49 (d, J = 8.0 Hz, 2H), 5.48 (s, 2H). ^{13}C NMR (100 MHz, Acetone-d_6) δ [ppm]: 157.18, 154.13, 151.78, 147.50, 147.37, 143.07, 136.68, 134.95, 133.69, 129.88, 128.74, 126.05, 123.75, 123.43, 121.17, 118.32, 113.82, 105.19, 70.23.

*4.1.5.22. 1-(6-(4-Chlorobenzyloxy)quinazolin-7-yl)-3-p-tolylurea (**27**).* Yield 73%; ^{1}H NMR (400 MHz, Acetone-d_6) δ [ppm]: 9.19 (s, 1H), 9.06 (s, 1H), 8.97 (s, 1H), 8.79 (s, 1H), 8.51 (s, 1H), 7.63 (d, J = 8.4 Hz, 2H), 7.59 (s, 1H), 7.49 (d, J = 8.4 Hz, 2H), 7.43 (d, J = 8.2 Hz, 2H), 7.12 (d, J = 8.2 Hz, 2H), 5.46 (s, 2H), 2.35 (s, 3H). HRMS (ES$^+$): *m/z* calculated for $C_{23}H_{19}ClN_4O_2$: 419.1275 [M+H]$^+$. Found 419.1287; 441.1095 [M+Na]$^+$. Found 441.1104.

*4.1.5.23. 1-(6-(4-Chlorobenzyloxy)quinazolin-7-yl)-3-(3-chlorophenyl)urea (**28**).* Yield 79%; ^{1}H NMR (400 MHz, DMSO-d_6) δ [ppm]: 9.96 (s, 1H), 9.26 (s, 1H), 9.08 (s, 1H), 8.84 (s, 1H), 8.74 (s, 1H), 7.78 (d, J = 1.8 Hz, 1H), 7.66 (s, 1H), 7.62 (d, J = 8.4 Hz, 2H), 7.51 (d, J = 8.4 Hz, 2H), 7.38–7.25 (m, 2H), 7.10–7.08 (m, 1H), 5.47 (s, 2H). HRMS (ES$^+$): *m/z* calculated for $C_{22}H_{16}Cl_2N_4O_2$: 461.0548 [M+Na]$^+$. Found 461.0375.

*4.1.5.24. 1-(6-(4-Chlorobenzyloxy)quinazolin-7-yl)-3-(3,4-dichlorophenyl)urea (**29**).* Yield 84%; ^{1}H NMR (400 MHz, DMSO-d_6) δ [ppm]: 10.05 (s, 1H), 9.26 (s, 1H), 9.08 (s, 1H), 8.85 (s, 1H), 8.74 (s, 1H), 7.94 (d, J = 2.5 Hz, 1H), 7.66 (s, 1H), 7.62 (d, J = 8.4 Hz, 2H), 7.56 (d, J = 8.8 Hz, 1H), 7.51 (d, J = 8.4 Hz, 2H), 7.35 (dd, J = 8.8, 2.5 Hz, 1H), 5.47 (s, 2H). HRMS (ES−): *m/z* calculated for $C_{22}H_{15}Cl_3N_4O_2$: 471.0183 [M−H]$^-$. Found 471.0176.

*4.1.5.25. 1-(6-(4-Chlorobenzyloxy)quinazolin-7-yl)-3-(3-fluorophenyl)urea (**30**).* Yield 77%; ^{1}H NMR (400 MHz, DMSO-d_6) δ [ppm]: 9.97 (s, 1H), 9.26 (s, 1H), 9.08 (s, 1H), 8.85 (s, 1H), 8.75 (s, 1H), 7.66 (s, 1H), 7.63 (d, J = 8.4 Hz, 2H), 7.57–7.54 (m, 1H), 7.52 (d, J = 8.4 Hz, 2H), 7.39–7.33 (m, 1H), 7.16 (d, J = 8.2 Hz, 1H), 6.86 (td, J = 8.2, 2.0 Hz, 1H), 5.48 (s, 2H). HRMS (ES$^+$): *m/z* calculated for $C_{22}H_{16}ClFN_4O_2$: 445.0844 [M+Na]$^+$. Found 445.0843.

*4.1.5.26. 1-(6-(4-Chlorobenzyloxy)quinazolin-7-yl)-3-(2-fluorophenyl)urea (**31**).* Yield 86%; ^{1}H NMR (400 MHz, Acetone-d_6) δ [ppm]: 9.20 (s, 1H), 9.07 (s, 1H), 9.04 (s, 1H), 8.98 (s, 1H), 8.76 (s, 1H), 8.34 (td, J = 8.3, 1.6 Hz, 1H), 7.63–7.59 (m, 3H), 7.47 (d, J = 6.7 Hz, 2H), 7.21–7.14 (m, 2H), 7.09–7.06 (m, 1H), 5.46 (s, 2H). HRMS (ES$^+$): *m/z* calculated for $C_{22}H_{16}ClFN_4O_2$: 423.1024 [M+H]$^+$. Found 423.1031; 445.0844 [M+Na]$^+$. Found 445.0854.

4.2. Evaluation of the biological activity

4.2.1. Cell culture

HT-22 (mouse hippocampal cells) cells were grown in Dulbecco's Modified Eagle's Medium (DMEM, GIBCO) supplemented with 10% (v/v) FBS and antibiotics (100 μg/mL penicillin/streptomycin mix) in a humidified atmosphere at 37 °C with 5% CO_2.

4.2.2. JC-1 mitochondrial membrane potential assay

HT-22 cells (30,000 per well) were seeded into a clear 96-well plate (FALCON) at 200 μL per well one day prior to assay. 750 μM of JC-1 (Stratagene) in DMSO stock solution was dissolved into

phenol red-free Opti-MEM (GIBCO) medium to make final concentration of 7.5 μM JC-1 per well. Medium was removed from the plate, and 100 μL per well of JC-1 was added. Plates were incubated for 1 h and 15 min at 37 °C and washed twice with 100 μL per well PBS. Subsequently, cells were treated with 25 μL solution of each compound at 5 μM in Opti-MEM and incubated at 37 °C for 10 min followed by addition of 25 μL of Aβ (American peptide, 1–42) solution at 5 μM. Fluorescence was measured at every 1 h for 3 h at ex/em 530 nm/580 nm ('red') and ex/em 485 nm/530 nm ('green'). The ratio of green to red fluorescence was recorded and the percent changes in ratio from each compound were calculated and normalized using vehicle control as 100%.

4.2.3. Cell viability MTT assay

5000 HT-22 cells per well were seeded and treated as above described method without adding Aβ. Cells were incubated at 37 °C for 24 h. 10 μL of MTT solution (3-(4,5-Dimethylthiazol-2-yl)-2,5-diphenyltetrazolium bromide, MTT, Sigma) was added directly to each well and incubated at 37 °C for 2 h. After confirming the formation of blue formazan precipitates under microscope, 140 mL of solubilizing solution (10% Triton-X 100 in isopropanol with 0.1 M HCl) was added to each well and incubate for another hour at room temperature. Absorbance at 570 nM was measured and OD values from each well were subtracted with vehicle control and cell viability was calculated.

4.2.4. Molecular docking

Ligand molecules preparation was performed in Maestro v.9.2, using OPLS2005 force field. Molecular modeling calculation and docking studies were carried out using GOLD docking program (Gold Suite-5.2) [20] using the X-ray crystal structure of CypD in complex with its inhibitor CsA (PDB ID: 2Z6W), 0.96 Å, from Protein Data Bank [21]. Docking was performed where all atoms were selected within 11 Å. CHEMPLP score, the current default fitness scoring function in Gold Suite-5.2, was used to assess the resulted docking poses.

Conflict of interest

The authors have declared no conflict of interest.

Acknowledgment

This work was funded by the KIST Institutional Programs (Grant No. 2E24760) from Korea Institute of Science and Technology (KIST), and by the Creative Fusion Research Program (Grant No. CAP-12-1) from Korea Research Council of Fundamental Science and Technology.

Our research team would like to thank Dr. Khalid B. Selim from (Faculty of pharmacy, Mansoura University, Egypt) for his invaluable assistance and helpful discussions. We appreciate to Dr. Hyun-Mee Park from (Advanced Analysis Center of Korea Institute of Science and Technology) for Mass Spectroscopy analysis. We also deeply acknowledge the editorial staff and the reviewers of this article for their great effort and time.

Appendix A. Supplementary data

Supplementary data related to this article can be found at http://dx.doi.org/10.1016/j.ejmech.2014.07.027.

References

[1] http://www.who.int/mediacentre/factsheets/fs362/en/index.html, in.
[2] L.O.N. White, H. Petrovitch, J. Hardman, J. Nelson, D.G. Davis, G.W. Ross, K. Masaki, L. Launer, W.R. Markesbery, Cerebrovascular pathology and dementia in autopsied Honolulu-Asia aging study participants, Ann. N. Y. Acad. Sci. 977 (2002) 9–23.
[3] Pathological correlates of late-onset dementia in a multicentre, community-based population in England and Wales. Neuropathology Group of the Medical Research Council Cognitive Function and Ageing Study (MRC CFAS), Lancet 357 (2001) 169–175.
[4] D. Aarsland, K. Andersen, J. Larsen, et al., The rate of cognitive decline in Parkinson disease, Arch. Neurol. 61 (2004) 1906–1911.
[5] A. Barker, M. Liddell, M.J. Owen, Role of amyloid β-protein in Alzheimer's disease, Lancet 340 (1992) 850–851.
[6] W. Cerpa, M.C. Dinamarca, N.C. Inestrosa, Structure-function implications in Alzheimer's disease: effect of Abeta oligomers at central synapses, Curr. Alzheimer Res. 5 (2008) 233–243.
[7] H. Du, L. Guo, F. Fang, D. Chen, A.A. Sosunov, G.M. McKhann, Y. Yan, C. Wang, H. Zhang, J.D. Molkentin, F.J. Gunn-Moore, J.P. Vonsattel, O. Arancio, J.X. Chen, S.D. Yan, Cyclophilin D deficiency attenuates mitochondrial and neuronal perturbation and ameliorates learning and memory in Alzheimer's disease, Nat. Med. 14 (2008) 1097–1105.
[8] P.H. Reddy, M.F. Beal, Amyloid beta, mitochondrial dysfunction and synaptic damage: implications for cognitive decline in aging and Alzheimer's disease, Trends Mol. Med. 14 (2008) 45–53.
[9] P. Bernardi, Mitochondrial transport of cations: channels, exchangers, and permeability transition, Physiol. Rev. 79 (1999) 1127–1155.
[10] A.A. Starkov, F.M. Beal, Portal to Alzheimer's disease, Nat. Med. 14 (2008) 1020–1021.
[11] C. Chinopoulos, A.A. Starkov, G. Fiskum, Cyclosporin a-insensitive permeability transition in brain mitochondria: inhibition by 2-aminoethoxydiphenyl borate, J. Biol. Chem. 278 (2003) 27382–27389.
[12] Z. Zhong, T.P. Theruvath, R.T. Currin, P.C. Waldmeier, J.J. Lemasters, NIM811, a mitochondrial permeability transition inhibitor, prevents mitochondrial depolarization in small-for-size rat liver grafts, Am. J. Transplant. 7 (2007) 1103–1111.
[13] M.W. Harding, R.E. Handschumacher, D.W. Speicher, Isolation and amino acid sequence of cyclophilin, J. Biol. Chem. 261 (1986) 8547–8555.
[14] J.-F. Guichou, J. Viaud, C. Mettling, G. Subra, Y.-L. Lin, A. Chavanieu, Structure-based design, synthesis, and biological evaluation of novel inhibitors of human cyclophilin A, J. Med. Chem. 49 (2006) 900–910.
[15] J. Kim, J. Lee, B. Moon, I. Mook-Jung, G. Nam, G. Keum, A.N. Pae, H. Choo, pyridyl-urea derivatives as blockers of Aβ-induced mPTP opening for Alzheimer's disease, Bull. Korean Chem. Soc. 33 (2012) 3887–3888.
[16] Y.S. Kim, S.h. Jung, B.-G. Park, M.K. Ko, H.-S. Jang, K. Choi, J.-H. Baik, J. Lee, J.K. Lee, A.N. Pae, Y.S. Cho, S.-J. Min, Synthesis and evaluation of oxime derivatives as modulators for amyloid beta-induced mitochondrial dysfunction, Eur. J. Med. Chem. 62 (2013) 71–83.
[17] A. Chilin, G. Marzaro, S. Zanatta, V. Barbieri, G. Pastorini, P. Manzini, A. Guiotto, A new access to quinazolines from simple anilines, Tetrahedron 62 (2006) 12351–12356.
[18] S.T. Smiley, M. Reers, C. Mottola-Hartshorn, M. Lin, A. Chen, T.W. Smith, G.D. Steele, L.B. Chen, Intracellular heterogeneity in mitochondrial membrane potentials revealed by a J-aggregate-forming lipophilic cation JC-1, Proc. Natl. Acad. Sci. 88 (1991) 3671–3675.
[19] B.K. Wagner, T. Kitami, T.J. Gilbert, D. Peck, A. Ramanathan, S.L. Schreiber, T.R. Golub, V.K. Mootha, Large-scale chemical dissection of mitochondrial function, Nat. Biotechnol. 26 (2008) 343–351.
[20] https://www.ccdc.cam.ac.uk/Solutions/GoldSuite/Pages/GOLD.aspx, in.
[21] http://www.rcsb.org/pdb/explore/explore.do?structureId=2Z6W, in.
[22] D.E. Clark, S.D. Pickett, Computational methods for the prediction of 'drug-likeness', Drug Discov. Today 5 (2000) 49–58.
[23] C.A. Lipinski, F. Lombardo, B.W. Dominy, P.J. Feeney, Experimental and computational approaches to estimate solubility and permeability in drug discovery and development settings, Adv. Drug Deliv. Rev. 23 (1997) 3–25.
[24] http://www.organic-chemistry.org/prog/peo/, in.
[25] I.V. Tetko, Computing chemistry on the web, Drug Discov. Today 10 (2005) 1497–1500.